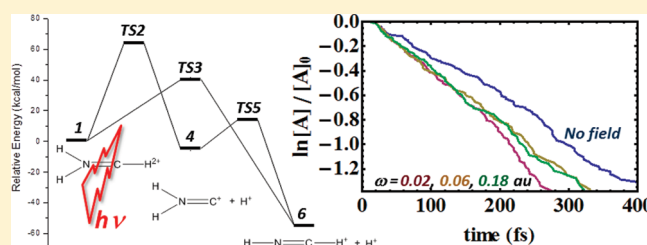


Dissociation of H_2NCH Dication in a Strong Laser Field

Jia Zhou and H. Bernhard Schlegel*

Department of Chemistry, Wayne State University, Detroit, Michigan 48202, United States

ABSTRACT: Ab initio classical molecular dynamics calculations have been used to simulate the dissociation of $\text{H}_2\text{NCH}^{2+}$ in a strong laser field. The frequencies of the continuous oscillating electric field were chosen to be $\omega = 0.02, 0.06,$ and 0.18 au (2280, 760, and 253 nm, respectively). The field had a maximum strength of 0.03 au (3.2×10^{13} W cm^{-2}) and was aligned with the CN bond. Trajectories were started with 100 kcal/mol of vibrational energy above zero point and were integrated for up to 600 fs at the B3LYP/6-311G(d,p) level of theory. A total of 200 trajectories were calculated for each of the three different frequencies and without a field. Two dissociation channels are observed: $\text{HNCH}^+ + \text{H}^+$ and $\text{H}_2\text{NC}^+ + \text{H}^+$. About one-half to two-thirds of the H^+ dissociations occurred directly, while the remaining indirect dissociations occurred at a slower rate with extensive migration of H^+ between C and N. The laser field increased the initial dissociation rate by a factor of ca. 1.4 and decreased the half-life by a factor of ca. 0.75. The effects were similar at each of the three frequencies. The $\text{HNCH}^+ \rightarrow \text{H}_2\text{NC}^+$ branching ratio decreased from 10.6:1 in the absence of the field to an average of 8.4:1 in the laser field. The changes in the rates and branching ratios can be attributed to the laser field lowering the reaction barriers as a result of a difference in polarizability of the reactant and transition states.



■ INTRODUCTION

Energized monocations and dications can be produced by short, intense laser pulses, and laser fields can further assist the dissociation of these ions. For a nonresonant laser field, singly and doubly charged molecules should interact more strongly than neutral molecules. In previous work,¹ we examined the potential energy surfaces for the unimolecular dissociation of CH_2NH neutral, monocation, dication, and trication in the absence of a laser field and used ab initio classical trajectory calculations to probe the molecular dynamics of the field-free dissociation process. In this paper, we present an initial study of the dissociation dynamics of $\text{H}_2\text{NCH}^{2+}$ in a strong laser field.

Interaction with an intense laser field can affect molecular reactions by altering their rates, branching ratios, and products' energy distributions. Coincident momentum imaging studies find that $\text{CH}_3\text{OH}^{2+}$ produced by short, intense laser pulses dissociates to $\text{CH}_3^+ + \text{HO}^+$, $\text{CH}_2^+ + \text{H}_2\text{O}^+$, and $\text{CH}^+ + \text{H}_3\text{O}^+$.^{2–6} Similar studies show that $\text{CH}_3\text{CN}^{2+}$ dissociates to $\text{CH}_3^+ + \text{CN}^+$, $\text{CH}_2^+ + \text{HCN}^+$, and $\text{CH}^+ + \text{H}_2\text{CN}^+$.⁷ Dissociation of allene dication created by intense laser pulses produces $\text{C}_3\text{H}_n^{2+}$, C_2H_n^+ , CH_n^+ , and H_n^+ ($n = 1–3$).^{8–11} In each of these cases, hydrogen migration competes with dissociation. For simple polyatomics, such as HCC^{2+} and $\text{H}_2\text{NCH}^{2+}$, simulations have shown that rearrangement occurs readily before dissociation even without a laser field.^{1,12}

The strong fields of a laser can interact directly with the charge, permanent dipole, and polarizability of a molecule. In the absence of resonant interactions and ionization, the oscillating electric field of a laser at IR and visible frequencies affects the potential energy surface primarily by polarizing the electronic distribution of a molecule via a nonresonant dynamic Stark effect

(for leading references, see ref 13). Strong laser field ionization and dissociation of H_2^+ and H_2 have been the subject of numerous accurate theoretical investigations (for example, see refs 14–21). The laser-driven dissociations of larger diatomics have been studied by classical, semiclassical, and quantum dynamics (for studies on HCl^+ , see refs 22–27). A few theoretical studies have examined laser-driven reactions of neutral polyatomic molecules and the vibrational dynamics of some ions (for some recent examples, see refs 28–36). However, for charged polyatomic molecules, there appear to be no computational studies of the effect of strong laser fields on the reaction rates and branching ratios. For laser intensities high enough to have a significant effect on the reaction dynamics, the nonlinear interaction with the field may be too strong to be handled by perturbation theory and, therefore, must be treated by direct simulation.

Our previous ab initio molecular dynamics study on the dissociation of energized methanimine dication ($\text{H}_2\text{NCH}^{2+}$) under field-free conditions showed that extensive hydrogen migration can occur before dissociation.¹ The major dissociation channels were $\text{HNCH}^+ + \text{H}^+$ and $\text{H}_2\text{NC}^+ + \text{H}^+$. For the energized dications, about two-thirds of the H^+ dissociations occurred directly, while the remaining dissociations occurred indirectly with extensive migration of H^+ between C and N. With an initial vibrational energy of 120 kcal/mol, the $\text{HNCH}^+ + \text{H}^+$ to $\text{H}_2\text{NC}^+ + \text{H}^+$ branching ratio was approximately 7:1. In the present paper, we report an initial study of the dissociation of

Received: May 7, 2011

Revised: June 20, 2011

Published: June 24, 2011

energized $\text{H}_2\text{NCH}^{2+}$ in a strong laser field and examined the effect of the oscillating electric field on the reaction rates, the $\text{HCNH}^+ + \text{H}^+$ to $\text{H}_2\text{NC}^+ + \text{H}^+$ branching ratio, and the fraction of direct versus indirect dissociations.

METHOD

The development version of the Gaussian suite of programs³⁷ was used for the ab initio electronic structure and molecular dynamics calculations. The geometries of the minima and the transition states without an electric field were optimized previously¹ with the B3LYP density functional^{38–40} and the 6-311G(d,p) basis set.⁴¹ This treatment was found to be in good agreement with CBS-APNO⁴² calculations for this system (MAD of 1.9 kcal/mol for the six structures in the present study). The unimolecular dissociation of $\text{H}_2\text{NCH}^{2+}$ in a laser field was simulated using ab initio molecular dynamics with and without an oscillating electric field. Classical trajectories were integrated using the velocity Verlet method⁴³ with a step size of 0.05 fs. At each time step, a fixed electric field of $\vec{\epsilon}(t_i) = \vec{\epsilon}_{\text{max}} \sin(\omega t_i)$ was applied, the adiabatic ground-state energy and gradients were computed with B3LYP/6-311G(d,p), and the displacements were calculated according to the velocity Verlet algorithm. The frequencies of the continuous wave (CW) laser field were chosen to be $\omega = 0.02, 0.06,$ and 0.18 au (2280, 760, and 253 nm, respectively). These frequencies are not in resonance with any of the fundamental vibrational frequencies of the ground state or any of the electronic excitation energies. To assess the maximal effect of the field on the barrier heights and branching ratio, the electric field was applied along the C–N bond axis. The electric field had a maximum strength of $\epsilon_{\text{max}} = 0.03$ au, corresponding to an intensity of $3.2 \times 10^{13} \text{ W cm}^{-2}$. This intensity is chosen to be high enough to have a noticeable effect on the reaction rates, but not so high as to cause significant ionization or excessive suppression of the barriers. The trajectories were initiated at the minimum energy geometry of the dication, $\text{H}_2\text{NCH}^{2+}$, and a microcanonical ensemble of initial states was constructed by normal mode sampling^{44,45} using the reactant vibrational frequencies calculated without a field. For practical reasons, the initial vibrational energy was adjusted so that most of the trajectories finished within a reasonable time. With a choice of 100 kcal/mol above zero point energy, ca. 85% of the trajectories finished within 600 fs. For each case (no field and $\omega = 0.02, 0.06,$ and 0.18 au), 200 trajectories were integrated for up to 600 fs (maximum of 12 000 steps) and were terminated when the minimum distance between fragments was greater than 10 bohr. To help interpret the trajectory results, the steepest descent reaction path in mass-weighted coordinates (the intrinsic reaction coordinate, IRC) was calculated in the absence of a field with the HPC method^{46,47} and the energies of points along the path were calculated at various fixed field strengths. Ratios of reaction rates were approximated by RRKM theory^{48,49} using the field-free reactant and transition-state harmonic vibrational frequencies and the estimated barriers with and without a field.

RESULTS AND DISCUSSION

The potential energy surface for the dissociation of $\text{H}_2\text{NCH}^{2+}$ was calculated previously¹ and is shown in Figure 1. $\text{H}_2\text{NCH}^{2+}$ (1) is the most stable structure of the dication. The lowest energy channel for dissociation of $\text{H}_2\text{NCH}^{2+}$ is loss of a proton to produce HCNH^+ (6, -55.3 kcal/mol) with a barrier of 41.5 kcal/mol (TS3). Loss of a proton to form H_2NC^+ (4) is less exothermic

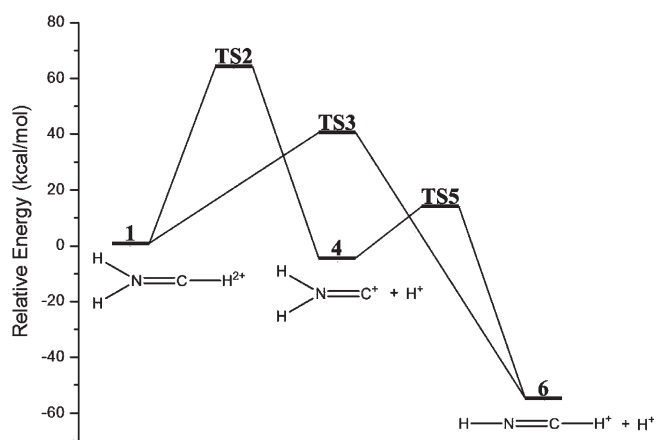


Figure 1. Relative energies for the dissociation of $\text{H}_2\text{NCH}^{2+}$ computed at the B3LYP/6-311G(d,p) level of theory.

Table 1. Number of Trajectories for the Dissociation of $\text{H}_2\text{NCH}^{2+}$ with and without an Oscillating Electric Field of 0.03 au

| | no field | $\omega = 0.02$ | $\omega = 0.06$ | $\omega = 0.18$ |
|--|----------|-----------------|-----------------|-----------------|
| $\text{HCNH}^+ + \text{H}^+$ direct dissociation | 71 | 105 | 67 | 72 |
| $\text{HCNH}^+ + \text{H}^+$ indirect dissociation | 77 | 66 | 73 | 85 |
| $\text{H}_2\text{NC}^+ + \text{H}^+$ direct dissociation | 11 | 17 | 20 | 15 |
| $\text{H}_2\text{NC}^+ + \text{H}^+$ indirect dissociation | 3 | 1 | 2 | 1 |
| no dissociation | 38 | 11 | 38 | 27 |

(-5.7 kcal/mol) and has a higher barrier (TS2, 63.6 kcal/mol). H_2NC^+ (4) can be converted to HCNH^+ (6) via TS5 with a barrier of 20.7 kcal/mol. These barriers calculated by B3LYP/6-311G(d,p) differ from the CBS-APNO values by less than 2 kcal/mol.¹

The results of the ab initio classical trajectory calculations are summarized in Table 1. For each of the four cases, 200 trajectories were started from the $\text{H}_2\text{NCH}^{2+}$ minimum using a microcanonical ensemble with an initial vibrational energy of 100 kcal/mol above zero point, distributed among the vibrational modes using normal mode sampling. The reactive trajectories can be classified into two types: (a) direct trajectories, characterized by H^+ dissociating without migrating from the atom to which it was initially bonded, and (b) indirect dissociations, characterized by H^+ migrating within the molecule before dissociating.

Without the field, 71 trajectories (35%) produced HCNH^+ directly, and 77 (39%) produced HCNH^+ indirectly. Only 14 trajectories out of 200 produced H_2NC^+ (5.5% direct and 1.5% indirect). There were also 36 trajectories (18%) that did not dissociate completely in the 600 fs simulation time and 2 trajectories that were discarded because of an energy conservation problem. This yields an $\text{HCNH}^+/\text{H}_2\text{NC}^+$ branching ratio of 10.6:1.

Three different frequencies were chosen for the laser field: 0.06 au (760 nm, approximately the Ti:sapphire laser frequency), a factor of 3 larger, and a factor of 3 smaller. When summed over the three frequencies, the number of indirect trajectories remained

Table 2. Half-Lives (fs) for the Dissociation of $\text{H}_2\text{NCH}^{2+}$ with and without an Oscillating Electric Field of 0.03 au

| | no field | $\omega = 0.02$ | $\omega = 0.06$ | $\omega = 0.18$ |
|--|----------|-----------------|-----------------|-----------------|
| all dissociation channels | 222 | 162 | 173 | 161 |
| HCNH ⁺ + H ⁺ direct dissociation | 153 | 109 | 91 | 101 |
| HCNH ⁺ + H ⁺ indirect dissociation | 278 | 228 | 236 | 241 |

about the same but the number of direct trajectories increased: 244 (41%) produce HCNH⁺ directly and 52 (8.7%) produced H_2NC^+ directly in the field, compared with 35% and 5.5% with no field. The branching ratio (direct + indirect) decreased from a field-free value of 10.6 to 8.4 in the laser field.

The effect of the laser field on the dissociation rates can be assessed by examining the half-life, $t_{1/2}$, for the various channels (Table 2). For the purpose of calculating the half-life, the dissociation is considered complete once the centers of mass of the fragments are 5 Å apart (the trends are not sensitive to the choice of this separation). For dissociation via both channels, the laser field decreases the half-life significantly. The effect is similar for the three frequencies considered and is also seen over somewhat longer times (e.g., $t_{3/4}$). The largest change in $t_{1/2}$ is seen for the HCNH⁺ direct channel, with the half-life decreasing by a factor of $1/3$. Because of the time required for the migration of H⁺ within the molecule, the half-lives for indirect HCNH⁺ + H⁺ dissociation are considerably longer than for the direct process. The effect of the laser field on the half-life for the indirect dissociation is smaller than for direct dissociation. The number of trajectories leading to H_2NC^+ + H⁺ products is too small to calculate meaningful half-lives.

More detailed information about the dissociation process can be obtained by examining the unimolecular reaction rates. These can be extracted from the trajectory data by plotting the logarithm of the fraction of undissociated trajectories versus time (Figure 2). The initial rates listed in Table 3 are obtained from the slopes of linear fits to the data from 0 to 300 fs (at later times, the plots are rather curved and have higher statistical uncertainties). Figure 2a and Table 3 show that the total dissociation rate is significantly greater in the field. For the first 200 fs, the rate is similar for the three frequencies. At later times, the rate with $\omega = 0.02$ au is somewhat greater than for $\omega = 0.06$ or 0.18 au. Because the indirect reactions involve extensive migration before dissociation, the rates for the indirect HCNH⁺ reaction are smaller than for the direct reaction (Figure 2, panel b vs panel c; Table 3). For $\omega = 0.02$ au at longer times, the indirect HCNH⁺ reaction shows a greater rate enhancement than the direct reaction. There are too few trajectories for the H_2NC^+ + H⁺ channel for a meaningful rate analysis. Table 3 indicates that the overall reaction rates in the field are a factor of 1.3–1.6 larger than without a field. The corresponding data for the HCNH⁺ direct and indirect channels show similar enhancements with the oscillating field. The average increase in the reaction rates in the laser field is 1.4. The greater rate enhancement seen for $\omega = 0.02$ au at longer times comes primarily from the indirect HCNH⁺ + H⁺ channel.

Some insight into the influence of a laser field on the unimolecular dissociation of $\text{H}_2\text{NCH}^{2+}$ can be obtained by examining the effect of an electric field on the potential energy surface. The intrinsic reaction coordinate (steepest descent path

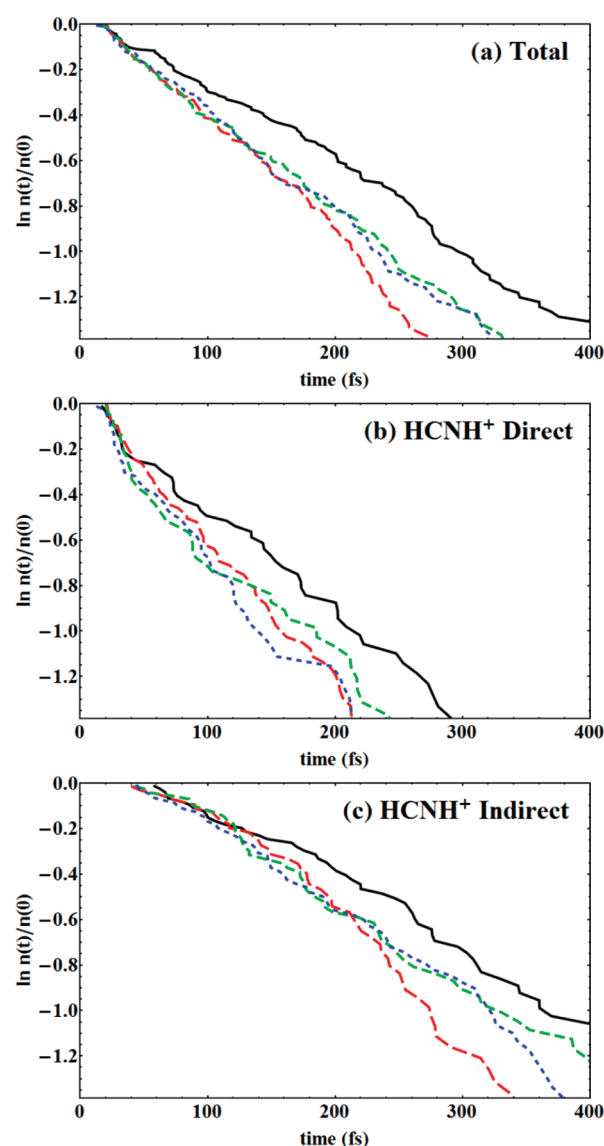


Figure 2. Unimolecular decomposition with and without an oscillating electric field. The rate is the negative of the slope of $\ln n(t)/n(0)$ versus time, where $n(t)/n(0)$ is the fraction of undissociated trajectories. (a) Total, (b) direct HCNH⁺ + H⁺, and (c) indirect HCNH⁺ + H⁺ with no field (black, solid), with a field of 0.03 au and $\omega = 0.02$ au (red, long dashes), $\omega = 0.06$ au (green, medium dashes), and $\omega = 0.18$ au (blue, short dashes).

Table 3. Dissociation Rates (ps^{-1}) for $\text{H}_2\text{NCH}^{2+}$ with and without an Oscillating Electric Field of 0.03 au

| | no field | $\omega = 0.02$ | $\omega = 0.06$ | $\omega = 0.18$ |
|--|----------|-----------------|-----------------|-----------------|
| all dissociation channels | 3.3 | 5.2 | 4.3 | 4.5 |
| HCNH ⁺ + H ⁺ direct dissociation | 4.6 | 6.5 | 5.6 | 6.6 |
| HCNH ⁺ + H ⁺ indirect dissociation | 2.8 | 4.6 | 3.8 | 3.5 |

in mass-weighted coordinates) was calculated in the absence of a field, and the energies for points along the path were determined by finite field calculations for various field strengths. Because translation of a charged molecule in a field changes its energy, the center of charge of the molecule (see below) was placed at the

Table 4. Static Polarizabilities (in au) for the Reactants, Transition States, and Products for $\text{H}_2\text{NCH}^{2+}$ Dissociation Calculated at the B3LYP/6-311G(d,p) Level of Theory

| | α_{xx} | α_{yy} | α_{yz} | α_{zz} | isotropic polarizability |
|--|---------------|---------------|---------------|---------------|--------------------------|
| $\text{H}_2\text{NCH}^{2+}$ | 6.99 | 9.59 | 0.00 | 18.43 | 11.67 |
| $\text{HCNH}^+ + \text{H}^+$ TS | 7.20 | 23.27 | 9.51 | 25.18 | 18.55 |
| $\text{HCNH}^+ + \text{H}^+$ product | 7.18 | 7.18 | 0.00 | 19.05 | 11.13 |
| $\text{H}_2\text{NC}^+ + \text{H}^+$ TS | 9.11 | 12.32 | 0.00 | 57.49 | 26.3 |
| $\text{H}_2\text{NC}^+ + \text{H}^+$ product | 9.47 | 12.83 | 0.00 | 17.60 | 13.3 |

origin. An electric field parallel to the CN bond of +0.03 au (negative near C and positive near N) and -0.03 au (positive near C and negative near N) has a large effect on the C–H distance in the $\text{H}_2\text{NCH}^{2+} \rightarrow \text{H}_2\text{NC}^+ + \text{H}^+$ transition state (ca. +0.5 and -0.5 Å, respectively) because the field is aligned with the breaking bond. However, this field has little effect on the N–H distance in the $\text{H}_2\text{NCH}^{2+} \rightarrow \text{HCNH}^+ + \text{H}^+$ transition state because the breaking bond is nearly perpendicular to the field. The energy of the transition state in the field was estimated by fitting a parabola to the three highest energy points along the path. A field of +0.03 and -0.03 au parallel to the CN bond lowers the calculated barrier by 1.9 and 1.6 kcal/mol for $\text{H}_2\text{NCH}^{2+} \rightarrow \text{HCNH}^+ + \text{H}^+$, and by 4.7 and 10.8 kcal/mol for $\text{H}_2\text{NCH}^{2+} \rightarrow \text{H}_2\text{NC}^+ + \text{H}^+$. Thus, the increase in the reaction rates can be attributed to the lowering of the barrier by the applied field, and the change in the branching ratio is due to the fact that one of the transition states is affected more strongly by the field.

The finite field energies can be compared to a Taylor series of the energy in terms of the dipole moment, $\vec{\mu}$; polarizability, α ; and hyperpolarizabilities, β , γ , etc.

$$E(\vec{\epsilon}(t)) = E(0) - \vec{\mu}\vec{\epsilon}(t) - \frac{1}{2}\alpha\vec{\epsilon}(t)^2 - \frac{1}{6}\beta\vec{\epsilon}(t)^3 - \frac{1}{24}\gamma\vec{\epsilon}(t)^4 \dots \quad (1)$$

For a charged molecule, the expectation value of the dipole moment operator

$$\vec{\mu} = \left\langle \psi \left| \sum_A Z_A \vec{R}_A - \sum_i^{\text{el}} \vec{r}_i \right| \psi \right\rangle = q\vec{R}_C \quad (2)$$

is equal to the net charge, q , times the position of the center of charge, \vec{R}_C . If the center of charge is placed at the origin, the dipole term is zero and the lowest order contribution is the polarizability term. The polarizabilities of the reactant and transition states listed in Table 4 can be employed to estimate the change in the barrier heights using $1/2(\alpha_{\text{TS}} - \alpha_{\text{reaction}})\vec{\epsilon}^2$. For the $\text{HCNH}^+ + \text{H}^+$ channel, the estimated lowering, 1.9 kcal/mol, is in good agreement with the values calculated in a finite field, 1.9 and 1.6 kcal/mol. However, the estimate of 11.0 kcal/mol for the $\text{H}_2\text{NC}^+ + \text{H}^+$ transition state does not compare quite as well with 4.7 and 10.8 kcal/mol obtained by the finite field calculations. This discrepancy and the large dependence on the direction of the field for the $\text{H}_2\text{NC}^+ + \text{H}^+$ channel is due to the very large hyperpolarizability for this transition state. If the system is free to rotate rather than being aligned with the field, the barrier lowering can be estimated using the isotropic polarizabilities. This yields an estimate of the rotationally averaged lowering of 2.5 and 7.1 kcal/mol for $\text{HCNH}^+ + \text{H}^+$ and $\text{H}_2\text{NC}^+ + \text{H}^+$, respectively, indicating that the change in the branching ratio

caused by the field should be less for the freely rotating system than for the aligned case.

Equation 1 is appropriate in the limit that the frequency of the oscillating field is small compared with the rate of the molecule passing through the transition state. Because it depends on the instantaneous field, the barrier lowering and the reaction rates should vary with the frequency of the field. In the high-frequency limit, the direction of the field changes many times while the molecule passes through the transition state, and it is necessary to average over the oscillation of the field. Integrating over one cycle yields the well-known result of $1/4\alpha\vec{\epsilon}_{\text{max}}^2$ for the energy lowering resulting from the polarizability (i.e., half the lowering of the low-frequency limit). The barrier lowering depends only on the maximum strength of the oscillating field and not on its frequency. In the high-frequency limit, the barriers for $\text{HCNH}^+ + \text{H}^+$ and $\text{H}_2\text{NC}^+ + \text{H}^+$ are lowered by 0.9 and 5.5 kcal/mol for the field aligned with the CN bond and by 1.2 and 3.5 kcal/mol for the rotationally averaged field. For the finite field calculations, averaging the energy lowering for four points in an optical cycle ($\vec{\epsilon} = \vec{\epsilon}_{\text{max}} \sin(\theta)$, $\theta = 0, \pi/2, \pi, 3\pi/2$) yields 0.9 and 3.9 kcal/mol for the barrier lowering for $\text{HCNH}^+ + \text{H}^+$ and $\text{H}_2\text{NC}^+ + \text{H}^+$, respectively.

The changes in the reaction rates due to the field-induced barrier lowering can be estimated using RRKM theory.^{48,49} This is only a rough estimate because the total energy is much greater than the barriers and the vibrational modes at these higher energies can be strongly anharmonic. With an initial energy of 100 kcal/mol above zero point, the branching ratio calculated by RRKM in the absence of an electric field is estimated to be 6.7 to 1 for $\text{HCNH}^+ + \text{H}^+$ versus $\text{H}_2\text{NC}^+ + \text{H}^+$. In the high-frequency limit, the laser field lowers the barriers by 0.9 and 3.9 kcal/mol, and RRKM theory estimates that the rates increase by a factor of 1.1 and 1.8, respectively, leading to a decrease in the branching ratio by a factor of 0.6. These changes are in qualitative agreement with the trajectory results.

CONCLUSIONS

Ab initio classical molecular dynamics calculations were used to simulate the dissociation of $\text{H}_2\text{NCH}^{2+}$ in a strong laser field. Frequencies of $\omega = 0.02, 0.06,$ and 0.18 au were chosen for the continuous oscillating electric field. For maximal effect, the electric field was aligned with the CN bond and had a maximum strength of 0.03 au. The reaction was given an initial energy of 100 kcal/mol above zero point. For the unimolecular decomposition of $\text{H}_2\text{NCH}^{2+}$ to $\text{HCNH}^+ + \text{H}^+$ and $\text{H}_2\text{NC}^+ + \text{H}^+$, one-half to two-thirds of the H^+ dissociations occurred directly, while the rest involved extensive migration of H^+ before dissociation. In the laser field, the half-life decreased by a factor of ca. 0.75 and the total dissociation rate during the first 300 fs increased by a factor of ca. 1.4. The effects were similar at each of the three frequencies. In the low-frequency limit, the barrier lowering depends on the instantaneous field strength, and thus, the rate should depend on the frequency of the field. However, in the high-frequency limit, the barrier lowering is due to the polarization averaged over the oscillations of the field, and the rate should be independent of the frequency. Even though the initial energy of $\text{H}_2\text{NCH}^{2+}$ is relatively high, the half-life of the dissociation is much larger than the period of oscillation of the electric field at each of the three frequencies, suggesting that the simulation corresponds to the high-frequency limit. The branching ratio for $\text{HCNH}^+ + \text{H}^+$ to $\text{H}_2\text{NC}^+ + \text{H}^+$ decreased from 10.6:1 in the absence of the field to

an average of 8.4:1 in the laser field as a result of the larger polarizability of the $\text{H}_2\text{NC}^+ + \text{H}^+$ transition state compared to the $\text{HNCH}^+ + \text{H}^+$ transition state.

AUTHOR INFORMATION

Corresponding Author

*E-mail: hbs@chem.wayne.edu.

ACKNOWLEDGMENT

This work was supported by a grant from the National Science Foundation (CHE0910858). Computer time on the Wayne State University grid is gratefully acknowledged.

REFERENCES

- (1) Zhou, J.; Schlegel, H. B. *J. Phys. Chem. A* **2009**, *113*, 9958.
- (2) Itakura, R.; Liu, P.; Furukawa, Y.; Okino, T.; Yamanouchi, K.; Nakano, H. *J. Chem. Phys.* **2007**, *127*, 104306.
- (3) Okino, T.; Furukawa, Y.; Liu, P.; Ichikawa, T.; Itakura, R.; Hoshina, K.; Yamanouchi, K.; Nakano, H. *Chem. Phys. Lett.* **2006**, *419*, 223.
- (4) Okino, T.; Furukawa, Y.; Liu, P.; Ichikawa, T.; Itakura, R.; Hoshina, K.; Yamanouchi, K.; Nakano, H. *Chem. Phys. Lett.* **2006**, *423*, 220.
- (5) Okino, T.; Furukawa, Y.; Liu, P.; Ichikawa, T.; Itakura, R.; Hoshina, K.; Yamanouchi, K.; Nakano, H. *J. Phys. B: At., Mol. Opt. Phys.* **2006**, *39*, S515.
- (6) Furukawa, Y.; Hoshina, K.; Yamanouchi, K.; Nakano, H. *Chem. Phys. Lett.* **2005**, *414*, 117.
- (7) Hishikawa, A.; Hasegawa, H.; Yamanouchi, K. *J. Electron Spectrosc. Relat. Phenom.* **2004**, *141*, 195.
- (8) Cornaggia, C. *Phys. Rev. A* **1995**, *52*, 4328.
- (9) Hoshina, K.; Furukawa, Y.; Okino, T.; Yamanouchi, K. *J. Chem. Phys.* **2008**, *129*, 104302.
- (10) Xu, H.; Okino, T.; Yamanouchi, K. *Chem. Phys. Lett.* **2009**, *469*, 255.
- (11) Xu, H. L.; Okino, T.; Yamanouchi, K. *J. Chem. Phys.* **2009**, *131*, 151102.
- (12) Li, X. S.; Schlegel, H. B. *J. Phys. Chem. A* **2004**, *108*, 468.
- (13) Townsend, D.; Sussman, B. J.; Stolow, A. *J. Phys. Chem. A* **2011**, *115*, 357.
- (14) Kawata, I.; Kono, H.; Fujimura, Y. *J. Chem. Phys.* **1999**, *110*, 11152.
- (15) Harumiya, K.; Kawata, I.; Kono, H.; Fujimura, Y. *J. Chem. Phys.* **2000**, *113*, 8953.
- (16) Harumiya, K.; Kono, H.; Fujimura, Y.; Kawata, I.; Bandrauk, A. D. *Phys. Rev. A* **2002**, *66*, 043403.
- (17) Uhlmann, M.; Kunert, T.; Grossmann, F.; Schmidt, R. *Phys. Rev. A* **2003**, *67*, 013413.
- (18) Kono, H.; Sato, Y.; Tanaka, N.; Kato, T.; Nakai, K.; Koseki, S.; Fujimura, Y. *Chem. Phys.* **2004**, *304*, 203.
- (19) Kono, H.; Sato, Y.; Kanno, M.; Nakai, K.; Kato, T. *Bull. Chem. Soc. Jpn.* **2006**, *79*, 196.
- (20) Uhlmann, M.; Grossmann, F.; Kunert, T.; Schmidt, R. *Phys. Lett. A* **2007**, *364*, 417.
- (21) Kato, T.; Kono, H.; Kanno, M.; Fujimura, Y.; Yamanouchi, K. *Laser Phys.* **2009**, *19*, 1712.
- (22) Thachuk, M.; Wardlaw, D. M. *J. Chem. Phys.* **1995**, *102*, 7462.
- (23) Thachuk, M.; Ivanov, M. Y.; Wardlaw, D. M. *J. Chem. Phys.* **1996**, *105*, 4094.
- (24) Thachuk, M.; Ivanov, M. Y.; Wardlaw, D. M. *J. Chem. Phys.* **1998**, *109*, 5747.
- (25) Paci, J. T.; Wardlaw, D. M.; Bandrauk, A. D. *J. Phys. B: At., Mol. Opt. Phys.* **2003**, *36*, 3999.
- (26) Paci, J. T.; Wardlaw, D. M. *J. Chem. Phys.* **2004**, *120*, 1279.
- (27) Korolkov, M. V.; Weitzel, K. M. *J. Chem. Phys.* **2005**, *123*, 164308.
- (28) Bandrauk, A. D.; Sedik, E. W. S.; Matta, C. F. *J. Chem. Phys.* **2004**, *121*, 7764.
- (29) Castro, A.; Marques, M. A. L.; Alonso, J. A.; Bertsch, G. F.; Rubio, A. *Eur. Phys. J. D* **2004**, *28*, 211.
- (30) Kawai, S.; Bandrauk, A. D.; Jaffe, C.; Bartsch, T.; Palacian, J.; Uzer, T. *J. Chem. Phys.* **2007**, *126*, 164306.
- (31) Bilalbegovic, G. *Eur. Phys. J. D* **2008**, *49*, 43.
- (32) Kawashita, Y.; Nakatsukasa, T.; Yabana, K. *J. Phys.: Condens. Matter* **2009**, *21*, 064222.
- (33) Taguchi, K.; Haruyama, J.; Watanabe, K. *J. Phys. Soc. Jpn.* **2009**, *78*, 094707.
- (34) Wang, Z. P.; Dinh, P. M.; Reinhard, P. G.; Suraud, E.; Zhang, F. S. *Int. J. Quantum Chem.* **2011**, *111*, 480.
- (35) Sato, Y.; Kono, H.; Koseki, S.; Fujimura, Y. *J. Am. Chem. Soc.* **2003**, *125*, 8019.
- (36) Nakai, K.; Kono, H.; Sato, Y.; Niitsu, N.; Sahnoun, R.; Tanaka, M.; Fujimura, Y. *Chem. Phys.* **2007**, *338*, 127.
- (37) Frisch, M. J.; Trucks, G. W.; Schlegel, H. B.; Scuseria, G. E.; Robb, M. A.; Cheeseman, J. R.; Scalmani, G.; Barone, V.; Mennucci, B.; Petersson, G. A.; Nakatsuji, H.; Caricato, M.; Li, X.; Hratchian, H. P.; Izmaylov, A. F.; Bloino, J.; Zheng, G.; Sonnenberg, J. L.; Hada, M.; Ehara, M.; Toyota, K.; Fukuda, R.; Hasegawa, J.; Ishida, M.; Nakajima, T.; Honda, Y.; Kitao, O.; Nakai, H.; Vreven, T.; Montgomery, J. A., Jr.; Peralta, J. E.; Ogliaro, F.; Bearpark, M.; Heyd, J. J.; Brothers, E.; Kudin, K. N.; Staroverov, V. N.; Kobayashi, R.; Normand, J.; Raghavachari, K.; Rendell, A.; Burant, J. C.; Iyengar, S. S.; Tomasi, J.; Cossi, M.; Rega, N.; Millam, N. J.; Klene, M.; Knox, J. E.; Cross, J. B.; Bakken, V.; Adamo, C.; Jaramillo, J.; Gomperts, R.; Stratmann, R. E.; Yazyev, O.; Austin, A. J.; Cammi, R.; Pomelli, C.; Ochterski, J. W.; Martin, R. L.; Morokuma, K.; Zakrzewski, V. G.; Voth, G. A.; Salvador, P.; Dannenberg, J. J.; Dapprich, S.; Daniels, A. D.; Farkas, Ö.; Foresman, J. B.; Ortiz, J. V.; Cioslowski, J.; Fox, D. J. *Gaussian Development Version*, revision H.X4 ed.; Gaussian, Inc.: Wallingford, CT, 2009.
- (38) Becke, A. D. *J. Chem. Phys.* **1993**, *98*, 1372.
- (39) Becke, A. D. *J. Chem. Phys.* **1993**, *98*, 5648.
- (40) Lee, C.; Yang, W.; Parr, R. D. *Phys. Rev. B* **1988**, *37*, 785.
- (41) Krishnan, R.; Binkley, J. S.; Seeger, R.; Pople, J. A. *J. Chem. Phys.* **1980**, *72*, 650.
- (42) Montgomery, J. A.; Ochterski, J. W.; Peterson, G. A. *J. Chem. Phys.* **1994**, *101*, 5900.
- (43) Swope, W. C.; Andersen, H. C.; Berens, P. H.; Wilson, K. R. *J. Chem. Phys.* **1982**, *76*, 637.
- (44) Hase, W. In *Encyclopedia of Computational Chemistry*; Schleyer, P. v. R., Allinger, N. L., Clark, T., Gasteiger, J., Kollman, P. A., Schaefer, H. F., III, Schreiner, P. R., Eds.; Wiley: Chichester, U.K., 1998; p 402.
- (45) Peshlherbe, G. H.; Wang, H.; Hase, W. L. *Adv. Chem. Phys.* **1999**, *105*, 171.
- (46) Hratchian, H. P.; Schlegel, H. B. *J. Chem. Phys.* **2004**, *120*, 9918.
- (47) Hratchian, H. P.; Schlegel, H. B. *J. Chem. Theory Comput.* **2005**, *1*, 61.
- (48) Marcus, R. A.; Rice, O. K. *J. Phys. Chem.* **1951**, *55*, 894.
- (49) Steinfeld, J. I.; Francisco, J. S.; Hase, W. L. *Chemical Kinetics and Dynamics*, 2nd ed.; Prentice Hall: Upper Saddle River, NJ, 1999.